Transactions of the 15th International Conference on
Structural Mechanics in Reactor Technology (SMiRT-15)
Seoul, Korea, August 15-20, 1999


# Thermal and Mechanical Behavior of Hemispherical Vessel Lower Head

K.Y. Suh[1], K.H. Kang[2], J.H. Kim[2], S.B. Kim[2], H.D. Kim[2], J.S. Cho[1] and J.E. Chang[1]

*1) Seoul National University, Korea*
*2) Korea Atomic Energy Research Institute, Korea*

## ABSTRACT

During a core melt accident, a potential for creating gap resistance and cooling was considered between the debris bed and the reactor vessel wall. In order to systematically investigate the potential for in-vessel debris cooling, a series of LAVA (Lower-plenum Arrested Vessel Attack) experiments are in progress at the Korea Atomic Energy Research Institute (KAERI). Currently proof-of-principle tests are being performed using the $Al_2O_3$/Fe thermite simulant. In these tests the influence of internal pressure load on the lower head vessel wall and the materials of the simulant melt on gap formation was investigated as well as the thermal behavior of the vessel. No indication of vessel failure was observed in any of the tests performed so far. In case the internal pressure was imposed, the lower head vessel experienced deformation at elevated temperatures and a thin gap formed around the interface between the solidified debris and the carbon steel vessel. The rapid cooling of the high temperature melt manifests the existence of a cooling mechanism of water ingression through the debris-to-vessel gap and the intra-debris pores and crevices. One- and two-dimensional analyses were performed for the ceramic/metal melt and the vessel to interpret the temperature history of the outer surface of the vessel wall measured from typical LAVA tests spanning heatup and cooldown periods.

## INTRODUCTION

The in-vessel cooling mechanism due to material creep and water ingression into the expanding gap between the debris and the vessel wall was found to explain the nonfailure of the Three Mile Island Unit 2 (TMI-2) reactor pressure vessel (PRV) lower head [1, 2]. With the success of the modeling effort, a research program SONATA-IV (Simulation of Naturally Arrested Thermal Attack in Vessel) had been developed to thoroughly investigate this inherent nature of degraded core coolability inside the lower head by Suh et al. [3, 4, 5, 6, 7, 8], whose engineering application was reported by Hwang at al. [9]. In addition to the natural mechanism for heat removal, the program has also pioneered newly engineered concepts of in- and ex-vessel gap cooling structures for advanced reactor designs [9].

## EXPERIMETAL DESCRIPTIONS

### Description of Tests

A schematic diagram of the LAVA experimental facility and the locations of the K-type thermocouples are shown in Figs. 1 and 2, respectively. The LHV (Lower Head Vessel) mockup made of carbon steel (SA516-Gr.70) consists of hemispherical and cylindrical parts with an inner diameter of 0.5 m and thickness of 0.025 m. Mixed $Al_2O_3$/Fe thermite melt or separated oxidic $Al_2O_3$ is used as corium simulant. In this paper five tests, LAVA-1,2,3,4 and 6 are documented as listed in Table 1.

Table 1. Experimental Conditions

| | LAVA-1 | LAVA-2 / LAVA-6 | LAVA-3 /LAVA-4 |
|---|---|---|---|
| Melt Mass & Composition | $Al_2O_3$/Fe, 40 kg | $Al_2O_3$/Fe, 40 kg | $Al_2O_3$, 30 kg |
| Water Mass & Initial Temp. | 70 kg, 418 K | 70 kg, 433 K | 70 kg, 430 K |
| In-/Ex-Vessel Pressure(MPa) | 1.74 / 1.74 | 1.75 / 0.1 | 1.7 / 0.1 |

### Summary of Test Results

The experimental results are summarized in Table 2. The post-test examination revealed the gap formation between the continuous solidified debris bed and the LHV wall. When the molten material is poured into the vessel filled with water, a gap originating from the contact resistance should be formed in the interface between the vessel and the solidified crust. Then the gap could be kept by the combined effect of the trapped water vaporization in the crevices of the LHV wall and the vessel expansion due to internal pressure and heatup. The internal pressure was considered to be a key factor in forming a gap on the molten iron metal layer that was highly superheated. On the other hand, the aluminum oxide layer easily formed the gap in all the cases, because of the differences in material property and the relatively low superheat of the aluminum oxide melt.

Table 2. Experimental Results

| Test | LAVA-1 | LAVA-2 | LAVA-3 | LAVA-4 | LAVA-6 |
|---|---|---|---|---|---|
| Melt Cooling Rate (K/s) | 6.6 | ** | 1.4 | 1.3 | 1.0 - 3.1 |
| LHV Max. Temp.(K) | 1517* | 1195* | 1224 | 1068 | 1365 |
| LHV Cooling Rate (K/s) | 0.24 | 0.25 | 0.29 - 0.52 | 1.28 - 4.38 | 0.3 |
| Gap Formation (Y/N) | No | Yes | Yes | Yes | Yes |
| LHV Deformation (mm) | ** | 2.7*** | 5.4 | 3.1 | ** |

* *Temperature at the 0° position was not measured.*

** *Information not available.*

*** *The measuring device was destroyed during the test.*

Temperature history of the LHV wall shows quite different thermal behavior depending on the experimental conditions. Figure 3 shows the comparison of the temperature histories of the LHV at the same latitude. In the LAVA-2 and LAVA-3 tests, the differences in the temperature increase rate and the maximum temperatures indicate the influence of the gap formation, but the characteristics of the vessel cool down were not changed compared with

the LAVA-1 test where no gap was formed. This result implies that there was no water ingression into the gap and to effectively cool down the RPV wall albeit a gap was formed. On the other hand, in the LAVA-4 test where the alumina was separated from the iron, a rapid cooling of the RPV wall was observed with a characteristic of quenching. The reason would be that the aluminum oxide layer is a highly porous debris bed with a large gap at the interface with the RPV wall. This gap will enable water to penetrate into the gap easily and allow steam to escape through fairly easily thus cooling the wall effectively.

## ANALYSIS OF TEST RESULTS

### One-Dimemsional Analysis

Computational model description

One-dimensional thermal analysis was performed for typical LAVA-2 and LAVA-4 LHV temperature measurements at 0°. The initial temperature of the molten alumina is assumed to be 2500 K and that of the LHV is 400 K. In the LAVA-4 test, the amount of the alumina is 30 kg. The grid meshes for the simplified one-dimensional analysis are 26 nodes in the alumina debris and 5 nodes in the carbon steel LHV.

For the simplified one-dimensional representation of alumina debris and the LHV shown in Fig. 4, the one-dimensional transient energy equation was formulated. In the LAVA-4 test, for instance, the porosity of the simulant was used to account for the difference between the volume of alumina with 100 % theoretical density (corresponding to calculated height of 0.106 m) versus the volume of alumina with the porosity (corresponding to the measured height of 0.125 m in the test). The properties were accordingly adjusted to accommodate for the pores within the debris assuming that the voids are filled with saturated steam.

The heat transfer takes place in the film boiling regime at the upper boundary. Berenson's correlation [10] is used accounting for the wave instability between the vapor and liquid phases. Film boiling heat transfer coefficients are employed when the temperature difference exceeds 100 K, while natural convection heat transfer coefficients are used below the temperature difference of 20 K. The intermediate region is treated as a transition region switching from the film boiling to the single phase heat transfer. In addition, the radiation heat transfer is considered. The heat transfer in the gap formed between alumina and the LHV is represented by a gap conductance and the heat transfer coefficient with which the heat is removed through the gap. The gap size is a pivotal parameter in this heat transfer calculation. Starting with a 0.1 mm gap and comparing with 1.0 mm and 10 mm gaps, for instance, one can check on the sensitivity of the gap conductance in the overall heat transfer calculation.

LAVA test simulation

In the LAVA-4 test, there forms initially a tiny gap of 1 μm which may expand up to 1 mm later on in the test. The water trapped in the gap is vaporized and expelled. The water is assumed to be supplied immediately to fulfill the continuity inside the gap. The gap cooling heat transfer coefficients are varied in the film boiling regime. Sensitivity studies were performed to gain insight into the multi-dimensional analysis. Figure 5 shows the effect of the initial gap size on the LHV thermal response. Note that the larger the initial gap, the slower the heatup rate of the LHV, which is well expected. Figure 6 examines the effect of varying gap size deformation with the fixed initial gap of 1 μm. It appears that the LHV thermal response is rather insensitive to the values chosen given the heat transfer coefficient of 1000 $W/m^2K$. The above results for the LAVA-4 LHV temperature at 0° generally demonstrate that the simple one-dimensional analysis indeed provides with reasonable

predictions spanning both the heatup and the cooldown periods.

Figure 7 compares the computed and measured thermal histories for the LAVA-2 LHV at 0°. In this case rather accelerated heatup rates are calculated from this one-dimensional analysis in which the iron settles down underneath the alumina debris due to density difference thereby enhancing the conductive and convective (due to high superheat) heat transfer to the LHV wall at an early stage. However, in the actual LAVA-2 test, some degree of mixing between the iron and alumina might have taken place in the leading edge at the time of relocation to and contact with the LHV wall. Use of mechanical mixture properties could certainly improve the agreement of the computed curve with that measured for LAVA-2.

**Two-Dimensional Analysis**

FLUENT model application

Computational fluid dynamics code FLUENT 4.32 [11] was used to simulate detailed transient two-dimensional thermal and flow distributions in the LAVA tests. FLUENT is a general-purpose computer program for modeling fluid flow, heat transfer, and chemical reaction. This code predicts the thermofluid phenomena by solving the conservation equations for mass, momentum and energy using a control volume based finite difference method. The unsteady turbulent two-dimensional basic equations for natural convection and heat transfer are solved using the SIMPLE algorithm and the power-law scheme in the curvilinear coordinates.

Numerical analyses are performed in a two-dimensional domain. The same material properties are consistently utilized for the alumina and iron debris as in the one-dimensional analysis. The calculation domain is limited to the molten pool and the LHV wall. The physical domain is of three-dimensional spherical configuration which is reduced to the rectangular coordinate using the grid transformation. The grid meshes are $36 \times 36$ nodes. The calculation domain and the physical grid domain are depicted in Fig. 8. The calculations were performed for the same LAVA-2 and LAVA-4 tests as had been treated by the simple one-dimensional approach in the previous section. The enthalpy method is used in FLUENT for modeling the phase change process.

In Fig. 8 (a), W1 through W4 delineate the boundaries of the calculational domain. Table 3 presents the applied condition to each boundary. W1 is the outer boundary surface of LHV which contacts with the atmosphere. This surface is exposed in the ambient air at 300 K. The surface boundary conditions are governed by the air natural convection and the radiation heat transfer. The air heat transfer coefficient $h_{air}$ is assumed to be 50, $\varepsilon_{ext}$ is the emissivity of the external surface and $\sigma$ is the Stefan-Boltzmann constant. In the equations above, $T_w$ and $T_\infty$ represent the boundary surface temperature and the ambient air temperature, respectively. W2 is the gap and W3 is the same height location as the debris pool height. On the W2 surface, heat transfer is considered in terms of the CHF (critical heat flux) and the radiation heat transfer. $T_{sat}$ is the saturation temperature at 2.0 MPa. The CHF is calculated from Monde et al.'s correlation [12]. The W3 boundary is given the conduction heat transfer. In Table 3, $k_{vs}$ is thermal conductivity of the LHV and L is the distance between W3 and top of the LHV. W4 denotes the upper surface of the debris covered with water, whose boundary condition is given by the film boiling and radiation heat transfer to the water.

Table 3. Boundary conditions for LAVA-2 and LAVA-4 in the two-dimensional calculation

| Boundary Surface | Boundary Condition |
|---|---|
| W1 | $q'' = h_{CHF}(T_w - T_{sat}) + \varepsilon_{ext}\sigma(T_w^4 - T_{sat}^4)$ |
| W2 | $q'' = h_{CHF}(T_w - T_{sat}) + \varepsilon_{ext}\sigma(T_w^4 - T_{sat}^4)$ |
| W3 | $q'' = \frac{k_{vx}}{L}(T_w - T_{sat})$ |
| W4 | $q'' = h_{film}(T_w - T_{sat}) + \varepsilon_{ext}\sigma(T_w - T_{sat})$ |

LAVA test simulation

In the LAVA-2 test the molten debris pool was stratified into a metal layer and an oxide layer on account of their density difference. The metal layer was located in the lower region in the test vessel. Unfortunately, however, the FLUENT code cannot calculate the multi-phase model and the phase-change model simultaneously. Therefore, the debris pool was assumed as homogeneous layer in this calculation. Figure 9 shows a comparison of the LAVA-2 experimental data and the numerical calculation results for the temperature history in the LHV. The comparison spot is located in the 2 mm depth and 0 degree of the LHV outer surface. In Fig. 9 the solid line represents the experimental data and the dotted lines signify calculation results. The first dotted line denotes the result of the case where the gap heat transfer is not considered, and the second dotted line expresses the result of the case where that 1 μm gap is assumed between the debris and the LHV. In the first case, the computed maximum temperature is higher than the measured one by as much as 300 K. For the case of 1 μm gap, the calculated maximum temperature is slightly lower than the measured one. On the other hand, the cooling rate of both calculations is higher than that of the test. This is probably because this calculation assumed that the debris is homogeneously mixed whereas in the test the metal layer was mostly located in the lower region.

For the LAVA-4 test, only an $Al_2O_3$ oxide pool was considered in this calculation as in the one-dimensional analysis. Assumption that initially there is a tiny gap (1 μm) was consistently applied as in the one-dimensional analysis. After 300 s it is assumed that a uniform 1 mm gap is formed. The W2 boundary condition is derived from Monde et al.'s CHF correlation [12]. Note, however, that this correlation may not directly be applied to the situation at hand since geometric and operating pressure conditions are different in the LAVA test from the correlation condition. This required sensitivity study to be performed for the CHF heat transfer. These values were varied from 100% to 25%. Figure 10 compares the LAVA-4 experimental data and the numerical calculation results for the temperature history in the LHV. The comparison spot is the same as in LAVA-2. Figure 10 illustrates that as the heat transfer coefficient in gap decreases, the calculation result approaches the LAVA test result. Figure 11 shows the numerical analysis results for (a) the flow pattern in the molten debris and (b) the temperature distribution at 90 s into the test. As shown in Fig. 11 (a), the debris pool solidifies from the upper boundary surface covered with water and from the gap between the debris and the LHV. The temperature varies fairly linearly within the crust region.

## CONCLUSION

Experiments were performed using $Al_2O_3$/Fe (or $Al_2O_3$ only) thermite melt to investigate the effects of the internal pressure load inside the vessel and of molten material on the gap formation and cooling of the test vessel wall. From the results of temperature history

measured in the LHV wall and visual examination of the structure inside the debris bed, it is inferred that a gap formed at the interface between the debris crust and LHV wall even in the iron layer when the internal pressure was imposed. This gap affected initial heatup of the vessel but could not necessarily ensure the cooling of the LHV wall. A significantly rapid temperature reduction occurred only in the $Al_2O_3$ thermite melt test, which is attributed to water penetrating into the gap and most effectively cooling the vessel. For clear confirmation of the inherent cooling mechanisms, the experiments will be performed with various initial conditions, especially the depth and the subcooling of water.

One- and two-dimensional analyses were performed for the ceramic/metal melt and the vessel to interpret the temperature history of the outer surface of the vessel wall measured from typical LAVA tests spanning heatup and cooldown periods. Both analyses demonstrated reasonable predictions of the temperature history of the LHV. The comparison sheds light on the thermal hydraulic and material behavior of the high temperature melt within the hemispherical vessel.

## REFERENCES


1. Suh, K.Y. and R.E. Henry, "Debris interactions in reactor vessel lower plena during a severe accident - I. Predictive model", *Nuclear Engineering & Design*, Vol. 166, 1996, pp. 147-163.
2. Suh, K.Y. and R.E. Henry, "Debris interactions in reactor vessel lower plena during a severe accident - II. Integral analysis", *Nuclear Engineering & Design*, Vol. 166, 1996, pp. 165-178.
3. Suh, K.Y., "SONATA-IV: Simulation Of Naturally Arrested Thermal Attack In Vessel - visualization study using Pyrex belljar and copper hemisphere heater", *presented at the Cooperative Severe Accident Research Program (CSARP) Semiannual Review Meeting*, Bethesda, MD, USA, May 1-5, 1995.
4. Suh, K.Y., C.K. Park and K.J. Yoo, "CAMPFIRE-2000: Comprehensive Accident Management Program Featuring Innovative Research & Engineering for the Year 2000 and Beyond", *presented at the OECD Specialist Meeting on Severe Accident Management Implementation*, Niantic, CT, USA, June 12-14, 1995.
5. Suh, K.Y., C.K. Park and K.J. Yoo, "In pursuit of naturally arrested thermal attack on reactor vessel during a severe accident, presented at the OECD-NEA CSNI PWG 4 & 2 Meetings", *Issy-les-Moulineaux*, France, September 26-29, 1995.
6. Suh, K.Y. and C.K. Park, "SONATA-IV: Simulation Of Naturally Arrested Thermal Attack In Vessel", *International Conference on Probabilistic Safety Assessment Methodology and Applications PSA'95*, Seoul, Korea, November 26-30, 1995.
7. Suh, K.Y., K.H. Bang and C.K. Park, "Inherent cooling of debris in reactor vessel and its implications for severe accident management", *International Conference on Probabilistic Safety Assessment and Management PSAM-III*, Crete, Greece, June 24-28, 1996.
8. Suh, K.Y. et al., "Melt-vessel gap coolability study within hemispherical lower plenum", *Nuclear Engineering & Design*, to appear, 1999.
9. Hwang, I.S. at al., "In-vessel retention against water reactor core melting accident", *Nucler Engineering & Design*, to appear, 1999.
10. Berenson, P.J., "Film-boiling heat transfer from a horizontal surface", *Journal of Heat Transfer*, Vol. 83, 1961, p. 351.
11. FLUENT 4.32 User's Guide, FLUENT Inc., Lebanon, NH, USA, January 1995.
12. Monde, M., H. Kusuda, and H. Uehara, "Critical heat flux during natural convective boiling in vertical rectangular channels submerged in saturated liquid", *Journal of Heat Transfer*, Vol. 104, 1982, pp. 300-303.

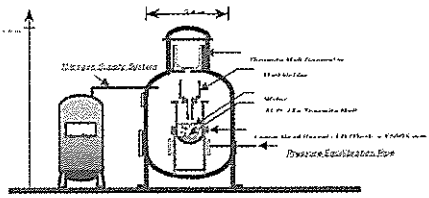

Fig. 1. Conceptual diagram of the LAVA experimental facility

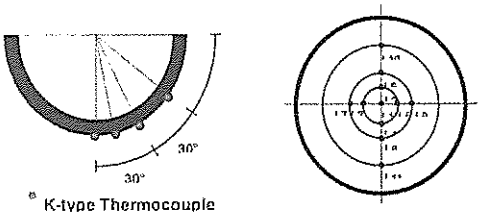


Fig. 2. Thermocouple locations on the lower head vessel surface

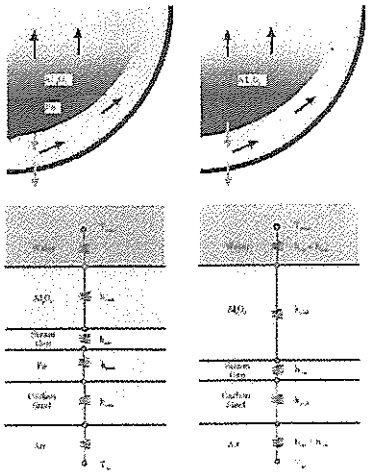

(a) LAVA-2 (b) LAVA-4

Fig. 4. One-dimensional representation of LAVA

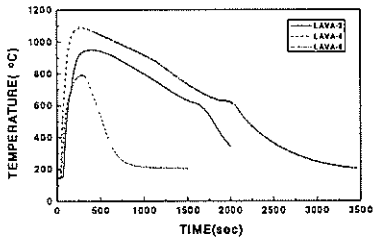


(a) 0° Positions

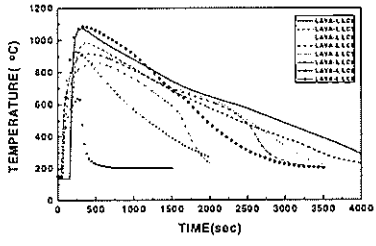


(b) 15° Positions

Fig. 3. Thermal behavior of the Lower Head Vessel

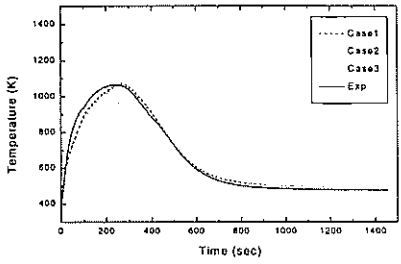


Fig. 5. Varying the initial gap size in LAVA-4

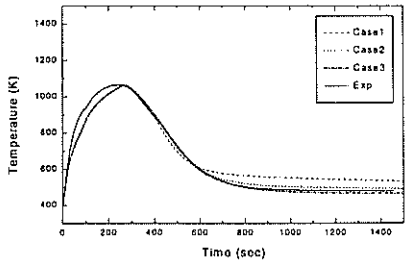


Fig. 6. Varying the deformed gap size in LAVA-4

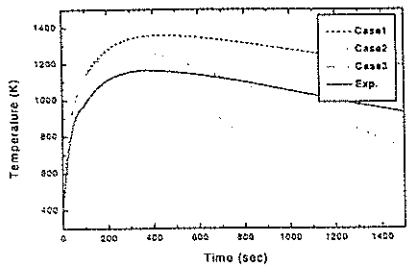


Fig. 7. Varying the gap parameters in LAVA-2

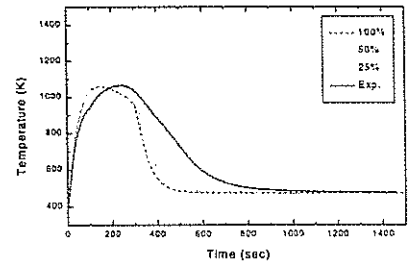


Fig. 10. Comparison of the temperature history with LAVA-4 test

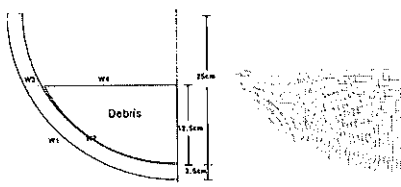


(a) Calculational domain (b) Physical grid

Fig. 8. Calculational domain and physical grid for LAVA simulation

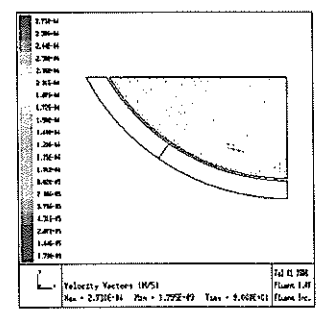

(a) Velocity vector

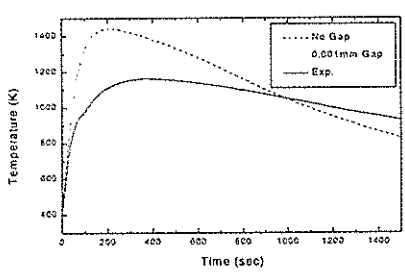


Fig. 9. Comparison of the temperature history with LAVA-2 test

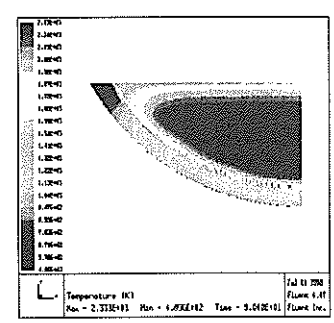

(b) Temperature profile

Fig. 11. FLUENT analysis results for the LAVA-4 test